


 Cite this: *RSC Adv.*, 2024, **14**, 18508

Synthesis and medicinal chemical characterisation of antiproliferative *O,N*-functionalised isopulegol derivatives†

 Tam Minh Le,^{ab} Isaac Kinyua Njangiru,^c Anna Vincze,^d István Zupkó,^c György T. Balogh^{*d} and Zsolt Szakónyi^{ID *a}

Benzylation of isopulegol furnished *O*-benzyl-protected isopulegol, which was transformed into aminodiols *via* epoxidation followed by ring opening of the corresponding epoxides and subsequent hydrogenolysis. On the other hand, (–)-isopulegol was oxidised to a diol, which was then converted into dibenzyl-protected diol derivatives. The products were then transformed into aminotriols by using a similar method. The antiproliferative activity of aminodiol and aminotriol derivatives was examined. In addition, structure–activity relationships were also explored from the aspects of substituent effects and stereochemistry on the aminodiol and aminotriol systems. The drug-likeness of the compounds was assessed by *in silico* and experimental physicochemical characterisations, completed by kinetic aqueous solubility and *in vitro* intestinal-specific parallel artificial membrane permeability assay (PAMPA-GI) measurements.

Received 10th May 2024

Accepted 2nd June 2024

DOI: 10.1039/d4ra03467h

rsc.li/rsc-advances

1 Introduction

Optically active aminodiols are of interest for the chiral pool and as partial structures of biologically active compounds.^{1–5} For example, their motif is found in the backbone of many bioactive molecules^{6–9} including pactamycin (antitumor),¹⁰ myriocin (antibiotic),¹¹ the proteasome inhibitor TMC-95A¹² and imino sugars,¹³ many of which are potent glycosidase inhibitors, just as miglustat and miglitol, which are in clinical development. In addition, the aminodiol subunit is present in several aza-sugars, polyhydroxylated indolizidine and pyrrolizidine alkaloids, many of which have interesting biological properties.^{14,15}

Furthermore, 2-amino-1,3-diol derivatives are common structural motifs present in nature. Relevant members of this family are sphingoid bases,¹⁶ sphinganines and clavaminol derivatives,^{17,18} which play important roles in physiological processes. In particular, sphingolipids,^{19,20} components of the cell membrane in living organisms, have been reported to be

involved in cell recognition and signal transduction,^{21,22} and they show antitumor,^{23,24} immune-modulatory²⁵ and immunosuppressive activities.^{26,27}

Besides pharmacological interests, aromatic and aliphatic aminodiols bearing a 1,2- or a 1,3-aminoalcohol moiety have proven to be useful building blocks materials in the stereoselective synthesis of compounds with pharmacological interest.^{28–30}

Besides their synthetic importance, aminodiols can also be applied as chiral ligands and auxiliaries in enantioselective transformation.^{31–33} In this regard, the asymmetric addition of organometallic reagents to aldehydes has become a highly investigated model reaction, applying chiral promoters such as 1,2- or 1,3-difunctionalised ligands.^{34–36}

Several chemical methods exist to produce 3-amino-1,2-diols, starting from chiral pool materials such as serine^{37–39} and glucose.⁴⁰ These include Sharpless asymmetric dihydroxylation with subsequent regioselective azide substitution,^{41,42} nucleophilic attack of α,β -epoxy carboxylic esters with azide followed by azide and ester reduction,⁴³ nonenzymatic one-pot synthesis of α,α' -dihydroxyketones *via* a mimetic of the transketolase reaction⁴⁴ and two-step stereoselective biocatalytic synthesis using a transketolase (TK) and a transaminase (TAm).⁴⁵ However, the most popular approaches to these motifs often employ the chiral pools utilising the stereospecific (e.g. Sharpless) epoxidation^{46–52} followed by C-3 regioselective ring-opening of 2,3-epoxy alcohols with amines.^{53–68} In the last decade, a metal- and solvent-free protocol,⁶⁹ involving C-3 selective ring-opening of 2,3-epoxy alcohols with amines catalysed by W-salts,⁷⁰ β -cyclodextrin,⁶⁶ $MgCl_2$,⁷¹ or the tungsten/

^aInstitute of Pharmaceutical Chemistry, University of Szeged, Eötvös utca 6, H-6720 Szeged, Hungary. E-mail: szakonyi.zsolt@szte.hu; Fax: +36 62 545705; Tel: +36 62 546809

^bHUN-REN-SZTE Stereochemistry, Research Group, University of Szeged, Eötvös u. 6, H-6720 Szeged, Hungary

^cInstitute of Pharmacodynamics and Biopharmacy, University of Szeged, H-6720, Eötvös utca 6, Szeged, Hungary

^dDepartment of Pharmaceutical Chemistry, Semmelweis University, Högyes Endre u. 9, H-1092 Budapest, Hungary

† Electronic supplementary information (ESI) available. See DOI: <https://doi.org/10.1039/d4ra03467h>



bis(hydroxamic acid) system⁷² as well as a two-step combined epoxidation/ring-opening methodology⁷³ were shown to generate virtually enantiopure functionalised 3-amino-1,2-diols. The ring-opening of chiral epoxy alcohols with nucleophiles^{74–82} provides direct access to versatile chiral building blocks for the synthesis of natural products and synthetic analogues with promising biological activities,^{83,84} such as cardiovascular,⁸⁵ antibacterial^{86,87} and sedative effects.⁸⁸

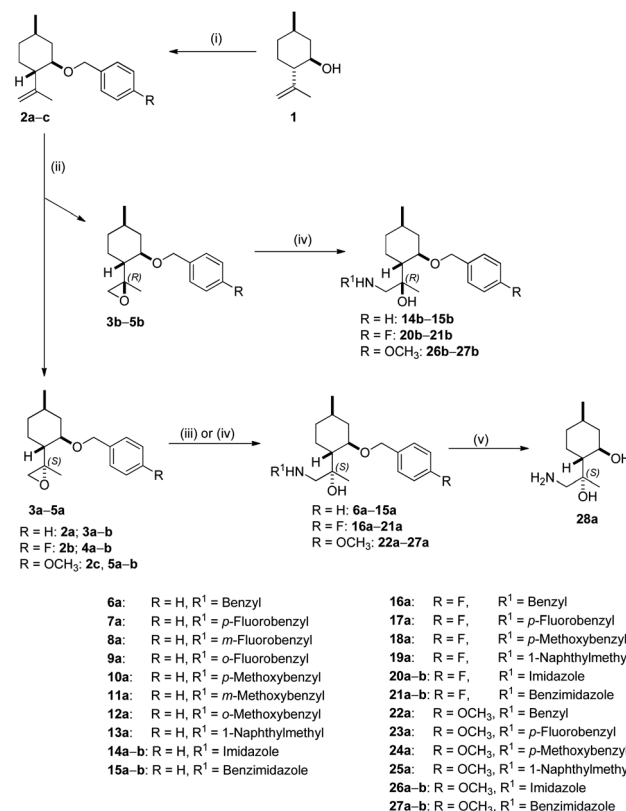
As a continuation of our research in structural modification of (–)-isopulegol for the development of anticancer agents,⁸⁹ we herein report the preparation of a new library of isopulegol-based chiral aminodiols and, as an extension, aminotriols *via* asymmetric epoxidation and aminolysis, starting from commercially available natural (–)-isopulegol. We have also carried out a preliminary study investigating the effect of stereochemistry and substitution level of the amine and hydroxyl functions on the antiproliferative activity on multiple human cancer cell lines. In addition to exploring the pharmacological effect, the medicinal properties of novel (–)-isopulegol derivatives have also been examined using *in silico* medchem-related parameters and early-stage *in vitro* screening assays on a panel of human cancer cells.

2 Results and discussion

2.1. Chemistry

Benzylation of isopulegol **1** produced *O*-benzyl isopulegol **2a**, which was subjected to epoxidation with *m*-CPBA to provide a 1 : 1 diastereomeric mixture of epoxides **3a** and **3b** in good yields. After chromatographic separation, ring opening of epoxide **3a** with different primary amines in the presence of LiClO₄ as catalyst delivered *O*-benzyl derivatives **6a–13a** in moderate to good yields. LiClO₄ shows enhanced reactivity for the ring-opening of epoxides through the coordination of Li⁺ with the epoxide oxygen, rendering the epoxide more susceptible to nucleophilic attack by amines and, therefore, dramatically reducing reaction times and improving yields.⁹⁰ Although ClO₄[–] can serve as an oxidative reagent, there is no oxidation under the applied condition. In addition to amines, the azole-mediated ring-opening of **3a** with a variety of azoles was also performed. In a similar fashion, the oxirane ring could only be opened in the presence of K₂CO₃ owing to the lower reactivity of *N*-containing heterocycles. A possible reaction pathway through K₂CO₃-promoted azole nucleophilicity and subsequent nucleophilic addition to epoxide **3a** afforded derivatives **14a** and **15a**.⁹¹ Debenzylation of **6a** by hydrogenolysis over Pd/C in MeOH resulted in primary aminodiol **28a** in moderate yields. The other epoxide **3b** underwent similar reactions. Interestingly, the oxirane ring-opening with azoles was successfully achieved, while aminolysis with primary amines did not take place under the applied conditions. This is probably due to steric hindrance exerted by both the benzyl and the methyl group at the α position in epoxide **3b**.⁹² The azole-based aminoalcohol adducts **14b** and **15b** were obtained with moderate yields (Scheme 1).

The literature revealed that various substituents of the benzyl group resulted in a significantly increased anticancer activity.⁹³ Therefore, benzylations were performed by utilising *p*-



Scheme 1 Isopulegol-based chiral aminodiol derivatives. Reagents and conditions: (i) NaH (1.0 eq.), substituted BnBr (1.5 eq.), KI (1.0 eq.), dry THF, 60 °C, 12 h, 70–88%; (ii) *m*-CPBA (2 eq.), Na₂HPO₄·12H₂O (3 eq.), CH₂Cl₂, 25 °C, 2 h, 25–47%; (iii) R¹NH₂ (2 eq.), LiClO₄ (1 eq.), CH₃CN, 70–80 °C, 20 h, 55–92%; (iv) imidazole or benzimidazole (3 eq.), K₂CO₃ (5 eq.), dry DMF, 70–80 °C, 96 h, 25–71%; (v) 5% Pd/C, H₂ (1 atm), CH₃OH, 25 °C, 24 h, 67–87%.

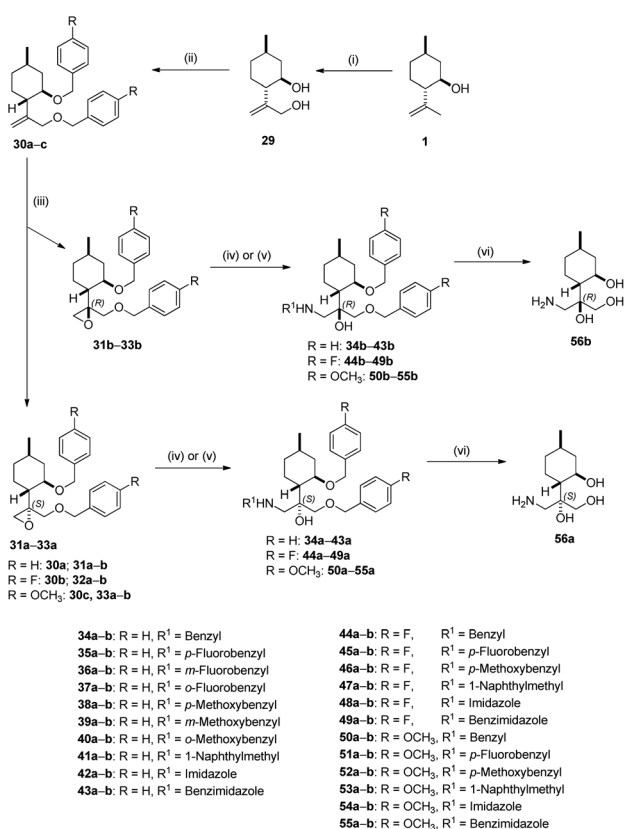
fluoro- and *p*-methoxybenzyl bromides as reagents. Benzyl-protected isopulegol **2b** and **2c** were formed in good yields. In the same manner, **2b** and **2c** afforded aminodiol derivatives **16–21** and **22–27** by the method described in Scheme 1. Aminodiols **16a** and **22a** were then transformed into primary aminodiol **28a** by hydrogenolysis over Pd/C. It has been reported that aminolysis and subsequent debenzylation gave the corresponding aminodiol with the same stereochemical configuration at the carbon atoms as that of the original moiety.⁹² The stereochemical structures of aminodiol **28a** is well-known in the literature,⁹² therefore, the absolute configuration of epoxide **3a–5a** could also be determined (Scheme 1).

Since the presence of the di-*O*-benzyl group could improve lipophilic properties leading to enhanced antiproliferative activity, derivative **30a** was synthesised.⁹⁴ However, the synthesis of **30a** starting from **2a** failed. Fortunately, we realised that it could be achieved starting from **29**, prepared from **1** by a three-step sequence including acetylation with Ac₂O/pyridine, followed by oxidation using SeO₂/*t*-BuOOH (TBHP) as oxidant and subsequent reduction with LiAlH₄.⁹⁵ Diol **29** smoothly transformed into di-*O*-benzyl derivative **30a** with an acceptable yield. Epoxidation of **30a** with *m*-CPBA produced a 1 : 1 mixture of epoxides **31a** and **31b**. After purification, ring opening of



oxirane **31a** was accomplished with different primary amines as well as azoles resulting in a library of aminoalcohols **34a–41a** and azole-based products **42a** and **43a**, respectively. Following this procedure, diastereoisomeric aminotriols **34b–41b** and **42b–43b** were prepared by ring opening of **31b** with primary amines and azoles. Primary aminotriols **56a** and **56b** was obtained by debenzylation of the corresponding aminotriols **34a** and **34b** by hydrogenation in the presence of a Pd/C catalyst under standard conditions (Scheme 2).

In order to study the effects of substituents of the benzyl group on antiproliferative properties, substituted di-*O*-benzyl derivatives with either electron-withdrawing or electron-donating substituents were obtained. When diol **29** were treated with either *p*-fluorobenzyl bromide or *p*-methoxybenzyl bromide in the presence of a catalytic amount of KI under reflux condition, product **30b** formed rapidly (24 h) in good yield, whereas longer reaction time (72 h) was required in the case of **30c**. The probable reason is steric hindrance exerted by the *p*-methoxybenzyl group of **30c** at the α position, which prevents the approach to the other hydroxyl group of the cyclohexyl ring.





Legend: Cancer cell growth inhibition: 20% or less (light red); Cancer cell growth inhibition: 100% (dark red)

Fig. 1 Antiproliferative activities of the *O,N*-functionalised (–)-isopulegol analogues against cancer cells. *: data from reference.⁹⁶

beyond the classical Lipinski rule of five (bRo5).⁹⁷ However, it is worth noting that in natural product-based drug research programmes it is not unusual to exploit the bRo5 space.⁹⁸ This, in our case, becomes particularly pronounced with *N*-benzyl *O*-benzyl aminodiol (**6a–30c**) and di-*O*-benzyl aminotriol (**34a–52b**) derivatives. The relationship between elevated lipophilicity and early ADME data can also be influenced by the basicity of the secondary amine moiety formed in the novel aminodiol-aminotriol derivatives, which can be identified on the basis of

the $pK_{a,\text{base}}$ values and $\log P - \log D_{7.4}$ differences. In our case, the unique behaviour of the bRo5-coupled physicochemical space is well reflected in the comparison of *in silico* parameters and *in vitro* characteristics. Regarding the lipophilicity values for neutral and ionic forms and the pK_a values describing the basic nature, no correlation can be drawn based on the kinetic aqueous solubility (kin.sol.) measured in a buffered system (PBS, pH 7.4) or the apparent permeability values (P_a) obtained in the phosphatidylcholine:cholesterol-based artificial lipid system (PAMPA, pH_{donor/acceptor} 7.4), which could be clearly interpreted. Thus, in contrast to weak kin.sol. and P_a values, identified in the case of derivatives with favourable physicochemical parameters (e.g. **6a**, **7a**, **14a–b**), several representatives of bRo5 also provided medium-high *in vitro* early ADME parameters (e.g. **8a**, **15a–b**, **39a–b**). In the latter case, the *N*-benzyl di-*O*-benzyl derivative group **44a–52b** should be mentioned as highlighted examples, where, in addition to the violation of the classic Ro5 (M_w and $\log P$),⁹⁹ the Veber's rule¹⁰⁰ (number of rotatable bond: nRot < 10 for good drug absorption) is also infringed, despite the fact that the kin.sol. and P_a values of these compounds are particularly high among all tested isopulegol derivatives.

Regarding the increased lipophilicity and general bRo5 nature of the tested isopulegol derivatives, it is also necessary to investigate separately their promiscuity risk and selectivity for individual cancer cell lines. In accordance, the compounds with an IC_{50} value less than 10 μM were evaluated and classified separately, according to their lipophilicity efficiency (LipE), which guides drug research programmes towards drug candidates that provide excellent *in vivo* efficacy and safety.¹⁰¹ As can be seen in Table 2, the 4-level classification system for both IC_{50} and LipE values proved to be sufficiently strict to identify selective and promiscuous isopulegol derivatives. Thus, it is particularly important to highlight compounds of our study that selectively provided a LipE value that was emphasised as a decreased (LipE >0.0) or moderate ($-0.5 < \text{LipE} \leq 0.0$) promiscuity risk. These criteria are met by two compounds of high potency (**10a**, **11a**) and one of low potency (**15a**) with high MCF-7 selectivity, which were identified as primary *in vivo* preclinical candidates. Compounds **12a** and **15b** showing HeLa and MCF-7 selectivity and compounds **36b** and **39a–b**, indicating MCF-7 and A2780 selectivity, were identified as secondary candidates with narrower selectivity and less favourable LipE values. Considering that several of the isopulegol derivatives showing selectivity also contain a methoxybenzyl moiety (**10a**, **11a**, **39a**), among the non-selective compounds with a high promiscuity risk, partial MCF-7 selectivity and sub-micromolar effect ($IC_{50} < 1 \mu\text{M}$), compounds **45a** and **46a** can be used for more detailed investigation as follow-up lead candidates. With a similar consideration, the partial selectivity of molecule **50b** for the A2780 cell line can be highlighted as an alternative candidate for further preclinical investigations.

2.4. Structure–activity relationship

The SARs of these novel derivatives were analysed and summarised. Compounds **34a–b** containing an *N*-benzyl-substituted aminoalcohol moiety showed enhanced antiproliferative activity



Table 1 Summary and classification for predicted physicochemical parameters and experimental early ADME data of isopulegol derivatives

Compounds	In silico parameters ^{a,b}				In vitro early ADME data ^d	
	M _w	pK _{a,base}	logP/logD _{7,4}	nRot ^c	Kinetic aqueous solubility(μM)	PAMPA permeability($P_a \times 10^{-6}$ cm s ⁻¹)
2a	244	—	5.2 / 5.2	4	1.1 ±0.01	ND*
2b	262	—	5.3 / 5.3	4	90 ±4.8	50.7 ±4.7
2c	274	—	5.2 / 5.2	5	247 ±2.8	26.1 ±5.4
6a	368	8.62	5.5 / 4.1	8	3.3 ±0.01	ND*
7a	386	8.58	5.3 / 4.0	8	2.5 ±0.1	ND*
8a	386	8.26	5.3 / 4.3	8	31.8 ±1.0	9.8 ±1.2
9a	386	7.92	5.3 / 4.6	8	1.4 ±0.02	ND*
10a	398	9.01	5.4 / 3.7	9	25.7 ±1.0	20.6 ±1.4
11a	398	8.52	5.4 / 4.2	9	82 ±2.2	1.8 ±0.5
12a	398	8.57	5.4 / 4.1	9	270 ±21	49.2 ±4.0
13a	418	8.28	6.3 / 5.3	8	2.1 ±0.1	ND*
14a	328	6.93	3.9 / 3.7	6	4.1 ±0.7	ND*
14b	328	6.93	3.9 / 3.7	6	3.7 ±0.7	ND*
15a	379	5.42	5.1 / 5.1	6	38.7 ±2.0	39.3 ±4.2
15b	379	5.42	5.1 / 5.1	6	34.6 ±1.1	26.3 ±4.6
30a	350	—	6.4 / 6.4	8	40.8 ±5.0	ND*
30b	386	—	6.7 / 6.7	8	17.6 ±0.6	ND*
30c	411	—	6.1 / 6.1	10	31.5 ±1.3	ND*
34a	474	8.16	6.8 / 5.8	12	2.8 ±0.2	ND*
34b	474	8.16	6.8 / 5.8	12	8.0 ±1.0	ND*
35a	492	8.12	6.8 / 5.9	12	1.1 ±0.1	ND*
35b	492	8.12	6.8 / 5.9	12	1.4 ±0.1	ND*
36a	492	7.79	6.8 / 6.2	12	20.9 ±1.7	ND*
36b	492	7.79	6.8 / 6.2	12	31.8 ±1.8	ND*
37a	492	7.46	6.8 / 6.4	12	2.6 ±0.2	ND*
37b	492	7.46	6.8 / 6.4	12	0.6 ±0.1	ND*
38a	504	8.55	6.6 / 5.3	13	3.2 ±0.1	ND*
38b	504	8.55	6.6 / 5.3	13	6.1 ±0.3	ND*
39a	504	8.06	6.6 / 5.8	13	40.9 ±1.7	7.5 ±0.3
39b	504	8.06	6.6 / 5.8	13	68.4 ±7.7	24.5 ±6.5

^a All *in silico* parameters were calculated by ACD/Labs Percepta: release 2023.1.1 (Build 3666, accessed on 4 Jul 2023, <https://www.acdlabs.com/products/percepta-platform>). ^b Classification system for *in silico* parameters: orange and red coloring indicates moderate and high violations of drug-likeness using Lipinski's⁹⁹ and Veber's¹⁰⁰ rules. ^c nRot – number of rotatable bonds. ^d Classification for experimental data: red – poor: kin.sol.≤10 μM, P_a : *ND (non-detectable compound at the acceptor site) – practically non-permeable; orange – moderate: 10 μM < kin.sol.≤ 50 μM or P_a ($\cdot 10^{-6}$ cm s⁻¹) ≤ 10; light green – high: 50 μM < kin.sol.≤ 100 μM or 10 < P_a ($\cdot 10^{-6}$ cm s⁻¹) ≤ 30; green – increased: kin.sol. >100 μM or P_a ($\cdot 10^{-6}$ cm s⁻¹) >30.



Table 1 (contd.)

Compounds	In silico parameters ^{a,b}				In vitro early ADMEda ^d	
	M _w	pK _{a,base}	logP/logD _{7.4}	nRot ^c	Kinetic aqueous solubility(μM)	PAMPA permeability(P _a × 10 ⁻⁶ cms ⁻¹)
40a	504	8.11	6.6 / 5.7	13	6.5 ±0.3	ND*
40b	504	8.11	6.6 / 5.7	13	1.6 ±0.1	ND*
41a	524	7.82	7.9 / 7.2	12	1.0 ±0.03	ND*
41b	524	7.82	7.9 / 7.2	12	0.5 ±0.01	ND*
42a	435	6.77	5.7 / 5.6	10	7.7 ±0.7	ND*
42b	435	6.77	5.7 / 5.6	10	5.2 ±0.3	ND*
43a	485	5.26	6.9 / 6.9	10	2.2 ±0.01	ND*
43b	485	5.26	6.9 / 6.9	10	1.6 ±0.1	ND*
44a	510	8.13	6.7 / 5.7	12	163 ±1.6	28.8 ±2.9
44b	510	8.13	6.7 / 5.7	12	97 ±2.8	23.2 ±2.7
45a	528	8.10	6.8 / 5.9	12	122 ±4.5	33.3 ±3.0
45b	528	8.10	6.8 / 5.9	12	197 ±2.3	22.7 ±0.8
46a	540	8.53	6.9 / 5.7	13	88 ±0.9	29.5 ±3.6
46b	540	8.53	6.9 / 5.7	13	172 ±3.4	27.4 ±1.6
50a	534	8.14	6.7 / 5.6	14	202 ±1.0	32.4 ±7.6
50b	534	8.14	6.7 / 5.7	14	92 ±0.9	34.0 ±4.0
51a	552	8.11	6.6 / 5.8	14	259 ±1.3	19.7 ±1.6
51b	552	8.11	6.6 / 5.8	14	124 ±5.9	33.2 ±3.3
52a	564	8.53	6.3 / 5.0	15	107 ±2.6	23.7 ±3.8
52b	564	8.53	6.3 / 5.0	15	117 ±2.9	37.4 ±3.5

compared with parent compound **30a**. This observation further confirms that the secondary amino scaffold seems to be needed for the pronounced activity, since analogues without these elements are considerably less effective. Introduction of substituents with electron-donating effect (OCH₃) into the *N*-benzyl ring could significantly improve the antiproliferative activity against most of the tested cancer cell lines (compared **34a-b** with **38a-b**), while compounds **35a-b** with electron-withdrawing character (F) at the *N*-benzyl ring showed slightly diminished antiproliferative effect compared with **34a-b**. This suggests that introduction of electron-donating substituents into the *N*-benzyl ring is beneficial and it improved *in vitro* antiproliferative activity. Compounds **39a-b**, where the benzene ring has a methoxy group in the *meta* position, was slightly better than analogues **40a-b** with the methoxy moiety at the *ortho* position. In contrast, switching the position of the methoxy substituent from the *ortho* to the *para* position (see compounds **38a-b**) reduced the inhibitory effect compared with **40a-b**, implying that the order of the activity was ranked as *meta* > *ortho* > *para*. Overall, electron-donating substituents at the *meta* position in the *N*-benzyl ring enhance activity. Replacement of the benzyl group (**34a-b**) by either a naphthylmethyl (**41a-b**) or an imidazole substituent (**42a-b**)

was detrimental for inhibitory activity against all tested cancer cell lines. Modification of the imidazole moiety in **42a-b** to benzimidazole (compounds **43a-b**) gave more potent but not outstanding molecules. Furthermore, there is no substantial difference in activity between **34a** and **34b** with different stereochemistry of the hydroxyl group on the alkyl chain. This demonstrates that the stereochemistry of the hydroxyl group in the aminodiol and aminotriol function has no influence on the antiproliferative effect. Introduction of the *O*-benzyl moiety with fluoro or methoxy substituent in compounds **46a-b** and **52a-b**, respectively, contributes to improve the antiproliferative effect compared to compounds **38a-b**, where R is hydrogen. However, compounds **46a-b** with a fluoro substituent in the *para* position of the *O*-benzyl rings were more potent than compounds **52a-b**, where the *O*-benzyl ring is *p*-methoxy-substituted. Taken together, these results demonstrate that the presence of electron-withdrawing R substituents of the *O*-benzyl moiety is beneficial and it improves *in vitro* antiproliferative activity. By contrast, replacing benzyl moieties in both **44a-b** and **50a-b** by either *p*-fluorobenzyl substituents (see **45a-b** and **51a-b**) or *p*-methoxybenzyl groups (see **45a-b** and **51a-b**) had no advantageous effects.



Table 2 Classification for antiproliferative effect and lipophilic efficiency of isopulegol derivatives

Compounds ^a	IC ₅₀ (μM) ^b /Lipophilic efficiency (LipE = pIC ₅₀ - logP) ^c			
	HeLa	MCF-7	MDA-MB-231	A2780
6a	2.8 / 0.09	2.3 / 0.18	3.4 / 0.01	2.6 / 0.12
7a	24.3 / —	20.3 / —	— / —	— / —
8a	5.2 / 0.00	3.5 / 0.17	9.9 / -0.28	9.3 / -0.25
9a	6.5 / -0.09	8.6 / -0.21	— / —	— / —
10a	4.3 / -0.03	1.9 / 0.32	5.7 / -0.15	7.3 / -0.25
11a	6.3 / -0.19	2.0 / 0.32	11.7 / —	12.5 / —
12a	4.6 / -0.05	4.2 / -0.01	12.8 / —	7.4 / -0.26
13a	5.4 / -1.04	4.3 / -0.94	25.0 / —	13.7 / —
14a	24.5 / —	— / —	— / —	— / —
14b	23.2 / —	— / —	— / —	— / —
15a	11.6 / —	7.0 / 0.02	16.7 / —	12.3 / —
15b	6.5 / 0.06	9.4 / -0.10	27.6 / —	10.9 / —
30a	— / —	— / —	— / —	— / —
30b	— / —	— / —	— / —	— / —
30c	24.7 / —	— / —	— / —	— / —
34a	2.6 / -1.16	2.0 / -1.05	4.0 / -1.35	4.1 / -1.36
34b	2.3 / -1.11	3.7 / -1.32	3.4 / -1.28	3.3 / -1.26
35a	7.2 / -1.66	10.4 / —	15.4 / —	11.9 / —
35b	2.5 / -1.21	2.6 / -1.22	3.8 / -1.39	4.3 / -1.44
36a	2.8 / -1.25	1.1 / -0.85	3.9 / -1.40	1.4 / -0.96
36b	2.3 / -1.18	0.74 / -0.68	4.2 / -1.43	0.91 / -0.77
37a	2.4 / -1.19	1.8 / -1.07	2.9 / -1.28	3.0 / -1.29
37b	2.6 / -1.22	5.1 / -1.52	6.0 / -1.59	4.0 / -1.41
38a	2.4 / -0.97	1.5 / -0.78	3.2 / -1.11	2.5 / -1.00
38b	2.4 / -0.98	2.1 / -0.93	3.2 / -1.10	3.8 / -1.18
39a	1.6 / -0.80	0.68 / -0.43	1.9 / -0.88	0.85 / -0.53
39b	4.6 / -1.27	1.5 / -0.77	16.8 / —	1.4 / -0.74
40a	2.1 / -0.91	1.8 / -0.85	2.5 / -0.99	2.2 / -0.94
40b	2.6 / -1.02	1.6 / -0.81	2.0 / -0.90	2.0 / -0.90
41a	2.6 / -2.28	5.9 / -2.64	3.6 / -2.42	5.0 / -2.57
41b	2.5 / -2.27	5.7 / -2.62	2.6 / -2.28	4.1 / -2.48
43a	6.9 / -1.69	7.5 / -1.72	12.4 / —	5.3 / -1.58
43b	4.0 / -1.45	5.7 / -1.60	5.0 / -1.55	4.3 / -1.49
44a	1.3 / -0.78	0.88 / -0.59	1.5 / -0.81	2.2 / -1.00
44b	3.0 / -1.12	0.96 / -0.63	2.7 / -1.08	2.1 / -0.97
45a	2.9 / -1.23	0.84 / -0.69	1.8 / -1.02	2.3 / -1.12
45b	2.7 / -1.20	0.91 / -0.73	1.9 / -1.05	1.4 / -0.92
46a	2.5 / -1.33	0.90 / -0.89	1.9 / -1.22	1.5 / -1.12
46b	1.6 / -1.14	0.90 / -0.89	1.8 / -1.19	1.4 / -1.08
50a	3.7 / -1.23	1.4 / -0.83	2.2 / -1.01	1.6 / -0.88
50b	3.1 / -1.16	1.5 / -0.84	2.1 / -1.00	0.93 / -0.64
51a	2.8 / -1.08	1.6 / -0.84	1.9 / -0.91	1.5 / -0.80
51b	3.6 / -1.19	1.3 / -0.75	3.2 / -1.13	1.9 / -0.91
52a	2.0 / -0.57	1.4 / -0.43	1.7 / -0.50	1.3 / -0.40
52b	3.5 / -0.83	1.6 / -0.48	2.8 / -0.73	1.5 / -0.46

^a Levels of *in vivo* preclinical candidate: green – primary candidates, orange – secondary candidates, red – representants of non-selective compounds. ^b Classification for antiproliferative effectivity: grey – non-/poorly effective at 30 and 10 μM test concentration or IC₅₀ > 10 μM; red – low: 6 μM ≤ IC₅₀ ≤ 10 μM; orange – moderate: 3 μM ≤ IC₅₀ < 6 μM; light green – high: 1 μM ≤ IC₅₀ < 3 μM; green – very-high: IC₅₀ < 1 μM.

^c Classification for LipE/promiscuity risk: purple – extreme risk: LipE ≥ -1.0, red – high risk: -1.0 < LipE ≤ -0.5, orange – moderate risk: -0.5 < LipE ≤ 0.0, light green – decreased risk: LipE > 0.0.

3 Experimental section

3.1. Chemistry

Commercially available solvents were used as obtained from suppliers (Molar Chemicals Ltd, Halásztelek, Hungary; Merck

Ltd, Budapest, Hungary and VWR International Ltd, Debrecen, Hungary), while applied solvents were dried according to standard procedures. Optical rotations were measured in MeOH at 20 °C with a PerkinElmer 341 polarimeter (PerkinElmer Inc., Shelton, CT, USA). Chromatographic separations and monitoring



of reactions were carried out on Merck Kieselgel 60 (Merck Ltd, Budapest, Hungary). Elemental analyses for all prepared compounds were performed on a PerkinElmer 2400 Elemental Analyzer (PerkinElmer Inc., Waltham, MA, USA). GC measurements for direct separation of commercially available enantiomers of isopulegol to determine the enantiomeric purity of starting material **1** and separation of *O*-acetyl derivatives of enantiomers were performed on a Chirasil-DEX CB column (2500 × 0.25 mm I.D.) on a PerkinElmer Autosystem XL GC consisting of a Flame Ionization Detector (PerkinElmer Corporation, Norwalk, CT, USA) and a Turbochrom Workstation data system (PerkinElmer Corp., Norwalk, CT, USA). Melting points were determined on a Kofler apparatus (Nagema, Dresden, Germany) and are uncorrected. ¹H- and ¹³C NMR were recorded on Brucker Avance DRX 500 spectrometer [500 MHz (¹H) and 125 MHz (¹³C), δ = 0 (TMS)]. Chemical shifts are expressed in ppm (δ) relative to TMS as the internal reference. *J* values are given in Hz.

(*–*)-Isopulegol **1** is available commercially from Merck Co with ee = 95%. Diol **27** were prepared according to literature procedures, and all spectroscopic data were similar to those described therein.^{95,102}

The detailed experimental process, physical and chemical characterisation and all spectroscopic data (¹H and ¹³C NMR together with HRMS) of new compounds can be found in the ESI.†

3.2. Physicochemical characterisation

L- α -Phosphatidylcholine (PC), cholesterol, phosphate buffered saline (PBS) powder and analytical grade solvents like DMSO, acetonitrile (AcN), dodecane, hexane and chloroform were purchased from Sigma Aldrich (Merck KGaA, Darmstadt, Germany). Phosphate buffered saline (PBS, pH 7.4) solutions were prepared by dissolving one bag of PBS powder in 1 L distilled water (provided by a Millipore Milli-Q® 140 Gradient Water Purification System). Donor buffer (pH 6.5) was made by mixing 0.01 M monosodium phosphate solution (0.01 M NaH₂PO₄, 0.0027 M KCl, 0.138 M NaCl) and 0.01 M disodium phosphate solution (0.01 M Na₂HPO₄, 0.0027 M KCl, 0.138 M NaCl) in a 3 : 1 ratio, and adjusting the pH with HCl.

3.2.1. Determination of kinetic aqueous solubility. Stock solutions were prepared from each compound in DMSO with the concentration of 10 mM. On a 96-well plate (Greiner PP) 15 μ L stock solution was pipetted into 285 μ L PBS (pH 7.4) to make kinetic solubility samples with the target concentration of 500 μ M. The plate was shaken for 2 hours at room temperature. After that the samples were transferred to a filter plate (MSSLBPC, Millipore, Merck KGaA, Darmstadt, Germany) and filtered by a vacuum-manifold (MultiScreen®HTS, Millipore, Merck KGaA, Darmstadt, Germany). Finally, the samples were diluted with AcN to prevent any precipitation. The samples were transferred to an UV-vis microplate (Greiner UV Star, Greiner Bio-One Hungary Kft, Budapest, Hungary) and absorbance data were collected on a wavelength range of 250–500 nm (1 nm stepsize) by a Multiskan Sky UV-vis plate reader (ThermoFisher Scientific Inc., Waltham, USA). Concentrations were calculated using a 3-point calibration at λ_{max} (absorbance maximum) for each compound.

3.2.2. Determination of intestinal-specific permeability by PAMPA. For the PAMPA assay, initial solutions were prepared with a nominal concentration of 500 μ M by mixing 15 μ L stock solution and 285 μ L donor buffer (pH 6.5) together. Each well of the acceptor plate (MSSACCEPTOR, reusable PTFE plate, Millipore, Merck KGaA, Darmstadt, Germany) were filled with 300 μ L acceptor buffer containing 5% DMSO (the same amount as in the donor phase). To prepare the artificial membrane, 16 mg L- α -phosphatidylcholine and 8 mg cholesterol were dissolved in 600 μ L solvent mixture (5 v/v% chloroform, 25 v/v% dodecane, 70 v/v% hexane) aided by sonication at 0 °C (Bandelin Sonorex Digitec, Bandelin electronic GmbH & Co. KG, Berlin, Germany). 5 μ L lipid solution was pipetted on each well of the donor plate (Multiscreen IP Filter plate, 0.54 μ m, Millipore, Merck KGaA, Darmstadt, Germany), then the plate was fitted into the prepared acceptor plate. After that, 150 μ Ls of the initial solutions were transferred to the wells of the donor plate. Finally, the plate sandwich was covered with a wet tissue paper and a plate lid to avoid evaporation of the solvent and incubated at 37 °C for 4 hours (Titramax1000, Heidolph Instruments GmbH & Co. KG, Schwabach, Germany). Finally, acceptor samples were transferred to an UV-vis microplate (Greiner UV Star, Greiner Bio-One Hungary Kft, Budapest, Hungary) and absorbance data were collected on a wavelength range of 250–500 nm (1 nm stepsize) by a Multiskan Sky UV-vis plate reader (ThermoFisher Scientific Inc., Waltham, USA).

For calculating the apparent permeability based on absorbance data, the following equation was used, described by Wohnsland and Faller.¹⁰³

$$P_a = -\frac{V_D \times V_A}{(V_D + V_A) \times A \times t} \times \ln(1 - r) \quad (1)$$

where P_a is the apparent permeability coefficient (cm s^{-1}), V_D and V_A are the volumes in the donor (0.15 cm^3) and acceptor phase (0.30 cm^3), A is the filter area (0.24 cm^2), t is the incubation time (14 400 s) and $r = \frac{[\text{Abs}]_{\text{Acceptor}}}{[\text{Abs}]_{\text{Equilibrium}}}$, where $[\text{Abs}]$ is the absorbance (at λ_{max}) of acceptor and equilibrium solutions. Equilibrium solutions were prepared by mixing 50 μ L initial solution and 100 μ L acceptor buffer together.

3.3. Determination of antiproliferative effect

The growth-inhibitory effects of the presented heterocyclic compounds were determined by a standard MTT (3-(4,5-dimethylthiazol-2-yl)-2,5-diphenyltetrazolium bromide) assay on a panel of human adherent cancer cell lines of gynecological origin containing HeLa (cervical cancers), A2780 (ovarian cancer), MCF7 and MDA-MB-231 (breast cancer) cells.¹⁰⁴ All cell lines were purchased from the European Collection of Cell Cultures (Salisbury, UK). The cells were cultivated in minimal essential medium (MEM) supplemented with fetal bovine serum (10%), non-essential amino acids, and penicillin-streptomycin (1% each) at 37 °C in a humidified atmosphere containing 5% CO₂. All media and supplements were obtained from Lonza Group Ltd (Basel, Switzerland). Cancer cells were plated into 96-well plates at 5000 cells per well density. After overnight incubation, the test compound was added in two concentrations (10 μ M and 30 μ M)



and incubated for 72 h under cell-culturing conditions. Then, MTT solution (5 mg mL⁻¹, 20 µL) was added to each well and incubated for four hours. Finally, the medium was removed, and the precipitated formazan was dissolved in DMSO during 60 min of shaking at 37 °C. The absorbance was measured at 545 nm using a microplate reader (SpectroStarNano, BMG Labtech, Ortenberg, Germany). Two independent experiments were carried out with five wells for each condition. In the case of the agents eliciting more than 50% cancer cell growth inhibition at 10 µM the assays were repeated with a broad range of concentration (0.1–30 µM) to obtain their IC₅₀ values. The clinically used anticancer agent cisplatin (Ebewe GmbH, Unterach, Austria) was included as a positive control. Calculations were performed using GraphPad Prism 5.01 software (GraphPad Software Inc., San Diego, CA, USA).

4 Conclusions

A new library of isopulegol-based chiral aminodiols and aminotriols was developed from commercially available (–)-isopulegol. Di-*O*-benzyl aminotriols have shown significant antiproliferative effectiveness in all tested cancer cell lines. Among these derivatives, *N*-benzyl-substituted di-*O*-benzyl aminodiol derivatives exert outstanding antiproliferative properties with low, typically micromolar IC₅₀ values.

Furthermore, *in vitro* studies have clearly shown that substitution of the *N*-benzyl ring with electron-donating groups could enhance antiproliferative activity, whereas the stereochemistry of hydroxyl substituent in the aminodiol and aminotriol function has no influence on the antiproliferative effect. Through SAR study, we also found that electron-withdrawing substituents on the *O*-benzyl moiety increase the *in vitro* antiproliferative potency.

The *in vitro* values demonstrated that compound **11a** has the potential to be developed into a clinically important therapeutic choice for the treatment of breast cancer.

Data availability

We declare that the data supporting this article have been included as part of the ESI† and available therein.

Author contributions

Z. S., I. Z. and G. T. B. conceived and designed the experiments; T. M. L, N. I. K and A. V. performed the experiments, analysed the data and wrote the experimental part; T. M. L, Z. S., I. Z. and G. T. B. discussed the results and contributed to write the paper. All authors have read and agreed to the published version of the manuscript.

Conflicts of interest

The authors declare no conflicts of interest.

Acknowledgements

We are grateful for financial support from the Hungarian Research Foundation (NKFI K138871). Project no. TKP2021-

EGA-32 has been implemented with the support provided by the Ministry of Innovation and Technology of Hungary from the National Research, Development and Innovation Fund, financed under the TKP2021-EGA funding scheme and also by University of Szeged Open Access Fund (grant No. 7057). The high-resolution mass spectrometric analysis was performed by Robert Berkecz. Project no. TKP2021-EGA-32 has been implemented with the support provided by the Ministry of Innovation and Technology of Hungary from the National Research, Development and Innovation Fund, financed under the TKP2021-EGA funding scheme.

References

- 1 D. Enders, A. Haertwig and J. Rumsink, *Eur. J. Org. Chem.*, 1998, **1998**, 1793–1802.
- 2 M. E. González-Rosende, J. M. Jordá-Gregori, J. Sepúlveda-Arques and M. Orena, *Tetrahedron: Asymmetry*, 2004, **15**, 419–422.
- 3 W. Guarneri, M. Sendzik, R. Fröhlich and D. Hoppe, *Synthesis*, 1998, 1274–1286.
- 4 A. Kamimura, K. Yoshihara, S. Marumo, A. Yamamoto, T. Nishiguchi, A. Kakehi and K. Hori, *J. Org. Chem.*, 1992, **57**, 5403–5413.
- 5 H. A. Walsh, P. L. Leslie, K. C. O'Shea and N. P. Botting, *Bioorg. Med. Chem. Lett.*, 2002, **12**, 361–363.
- 6 S. Hanessian, U. Soma, S. Dorich and B. Deschênes-Simard, *Org. Lett.*, 2011, **13**, 1048–1051.
- 7 A. Ohsaki, H. Ishiyama, K. Yoneda and J. Kobayashi, *Tetrahedron Lett.*, 2003, **44**, 3097–3099.
- 8 H. C. Kim and S. H. Kang, *Angew. Chem.*, 2009, **121**, 1859–1861.
- 9 M. Azumi, K. Ogawa, T. Fujita, M. Takeshita, R. Yoshida, T. Furumai and Y. Igarashi, *Tetrahedron*, 2008, **64**, 6420–6425.
- 10 J. T. Malinowski, R. J. Sharpe and J. S. Johnson, *Science*, 2013, **340**, 180–182.
- 11 M. C. Jones and S. P. Marsden, *Org. Lett.*, 2008, **10**, 4125–4128.
- 12 B. K. Albrecht and R. M. Williams, *Proc. Natl. Acad. Sci. U.S.A.*, 2004, **101**, 11949–11954.
- 13 R. J. Nash, A. Kato, C.-Y. Yu and G. W. Fleet, *Future Med. Chem.*, 2011, **3**, 1513–1521.
- 14 K. Burgess and I. Herderson, *Tetrahedron*, 1992, **48**, 4045–4066.
- 15 J. P. Michael, *Nat. Prod. Rep.*, 2001, **18**, 520–542.
- 16 S. T. Pruett, A. Bushnev, K. Hagedorn, M. Adiga, C. A. Haynes, M. C. Sullards, D. C. Liotta and A. H. Merrill, *J. Lipid Res.*, 2008, **49**, 1621–1639.
- 17 A. Aiello, E. Fattorusso, A. Giordano, M. Menna, C. Navarrete and E. Muñoz, *Tetrahedron*, 2009, **65**, 4384–4388.
- 18 T. Vijai Kumar Reddy, A. Jyotsna, B. L. A. Prabhavathi Devi, R. B. N. Prasad, Y. Poornachandra and C. Ganesh Kumar, *Eur. J. Med. Chem.*, 2016, **120**, 86–96.
- 19 T. Nakamura and M. Shiozaki, *Tetrahedron*, 2001, **57**, 9087–9092.



20 Y. A. Hannun and L. M. Obeid, *J. Biol. Chem.*, 2002, **277**, 25847–25850.

21 A. J. Dyckman, *J. Med. Chem.*, 2017, **60**, 5267–5289.

22 M. P. Wymann and R. Schneiter, *Nat. Rev. Mol. Cell Biol.*, 2008, **9**, 162–176.

23 J. Newton, S. Lima, M. Maceyka and S. Spiegel, *Exp. Cell Res.*, 2015, **333**, 195–200.

24 C. Huang and C. Freter, *Int. J. Mol. Sci.*, 2015, **16**, 924–949.

25 L. M. Healy and J. P. Antel, *Curr. Drug Targets*, 2016, **17**, 1841–1850.

26 L. Cavone, R. Felici, A. Lapucci, D. Buonvicino, S. Pratesi, M. Muzzi, B. Hakiki, L. Maggi, B. Peruzzi, R. Caporale, F. Annunziato, M. P. Amato and A. Chiarugi, *Brain, Behav., Immun.*, 2015, **50**, 78–86.

27 S. Ladisch, R. Li and E. Olson, *Proc. Natl. Acad. Sci. U. S. A.*, 1994, **91**, 1974–1978.

28 V. A. Pavlov, *Tetrahedron*, 2008, **64**, 1147–1179.

29 E. Gómez-Torres, D. A. Alonso, E. Gómez-Bengoa and C. Nájera, *Org. Lett.*, 2011, **13**, 6106–6109.

30 X.-P. Hui, C. Yin, Z.-C. Chen, L.-N. Huang, P.-F. Xu and G.-F. Fan, *Tetrahedron*, 2008, **64**, 2553–2558.

31 A. L. Braga, R. M. Rubim, H. S. Schrekker, L. A. Wessjohann, M. W. G. de Bolster, G. Zeni and J. A. Sehnem, *Tetrahedron: Asymmetry*, 2003, **14**, 3291–3295.

32 A. Vidal-Ferran, A. Moyano, M. A. Pericàs and A. Riera, *J. Org. Chem.*, 1997, **62**, 4970–4982.

33 C. Yie-Jia, J.-M. Fang and Ta-J. Lu, *Tetrahedron: Asymmetry*, 1995, **6**, 89–92.

34 R. Roudeau, D. Gomez Pardo and J. Cossy, *Tetrahedron*, 2006, **62**, 2388–2394.

35 I. Philipova, V. Dimitrov and S. Simova, *Tetrahedron: Asymmetry*, 1999, **10**, 1381–1391.

36 A.-L. Zhang, L.-W. Yang, N.-F. Yang and D.-C. Liu, *J. Organomet. Chem.*, 2014, **768**, 50–55.

37 G. Veerisa and A. Datta, *Tetrahedron Lett.*, 1998, **39**, 8503–8504.

38 A. J. Ndakala, M. Hashemzadeh, R. C. So and A. R. Howell, *Org. Lett.*, 2002, **4**, 1719–1722.

39 H. Azuma, S. Tamagaki and K. Ogino, *J. Org. Chem.*, 2000, **65**, 3538–3541.

40 V. D. Chaudhari, K. S. Ajish Kumar and D. D. Dhavale, *Org. Lett.*, 2005, **7**, 5805–5807.

41 L. He, H.-S. Byun and R. Bittman, *J. Org. Chem.*, 2000, **65**, 7627–7633.

42 K. Smithies, M. E. B. Smith, U. Kaulmann, J. L. Galman, J. M. Ward and H. C. Hailes, *Tetrahedron: Asymmetry*, 2009, **20**, 570–574.

43 T. Takanami, H. Tokoro, D. Kato, S. Nishiyama and T. Sugai, *Tetrahedron Lett.*, 2005, **46**, 3291–3295.

44 M. E. B. Smith, K. Smithies, T. Senussi, P. A. Dalby and H. C. Hailes, *Eur. J. Org. Chem.*, 2006, **2006**, 1121–1123.

45 M. E. B. Smith, B. H. Chen, E. G. Hibbert, U. Kaulmann, K. Smithies, J. L. Galman, F. Baganz, P. A. Dalby, H. C. Hailes, G. J. Lye, J. M. Ward, J. M. Woodley and M. Micheletti, *Org. Process Res. Dev.*, 2010, **14**, 99–107.

46 T. Katsuki and V. Martin, in *Organic Reactions*, ed. John Wiley & Sons, Inc., Hoboken, NJ, USA, 1996, pp. 1–299.

47 E. M. McGarrigle and D. G. Gilheany, *Chem. Rev.*, 2005, **105**, 1563–1602.

48 O. A. Wong and Y. Shi, *Chem. Rev.*, 2008, **108**, 3958–3987.

49 T. Katsuki and K. B. Sharpless, *J. Am. Chem. Soc.*, 1980, **102**, 5974–5976.

50 W. Zhang, A. Basak, Y. Kosugi, Y. Hoshino and H. Yamamoto, *Angew. Chem., Int. Ed.*, 2005, **44**, 4389–4391.

51 H. Egami, T. Oguma and T. Katsuki, *J. Am. Chem. Soc.*, 2010, **132**, 5886–5895.

52 J. L. Olivares-Romero, Z. Li and H. Yamamoto, *J. Am. Chem. Soc.*, 2013, **135**, 3411–3413.

53 R. M. Hanson, *Chem. Rev.*, 1991, **91**, 437–475.

54 P. Pena and S. Roberts, *Curr. Org. Chem.*, 2003, **7**, 555–571.

55 M. Caron and K. B. Sharpless, *J. Org. Chem.*, 1985, **50**, 1557–1560.

56 C. H. Behrens and K. B. Sharpless, *J. Org. Chem.*, 1985, **50**, 5696–5704.

57 S. Y. Ko and K. B. Sharpless, *J. Org. Chem.*, 1986, **51**, 5413–5415.

58 M. Caron, P. R. Carlier and K. B. Sharpless, *J. Org. Chem.*, 1988, **53**, 5185–5187.

59 M. Onaka, K. Sugita, H. Takeuchi and Y. Izumi, *J. Chem. Soc., Chem. Commun.*, 1988, 1173.

60 M. Canas, M. Poch, X. Verdaguer, A. Moyano, M. A. Pericàs and A. Riera, *Tetrahedron Lett.*, 1991, **32**, 6931–6934.

61 M. Chini, P. Crotti, L. A. Flippin, C. Gardelli, E. Giovani, F. Macchia and M. Pineschi, *J. Org. Chem.*, 1993, **58**, 1221–1227.

62 M. Sasaki, K. Tanino and M. Miyashita, *Org. Lett.*, 2001, **3**, 1765–1767.

63 M. Sasaki, K. Tanino, A. Hirai and M. Miyashita, *Org. Lett.*, 2003, **5**, 1789–1791.

64 M. Pastó, B. Rodríguez, A. Riera and M. A. Pericàs, *Tetrahedron Lett.*, 2003, **44**, 8369–8372.

65 Y. Tomata, M. Sasaki, K. Tanino and M. Miyashita, *Tetrahedron Lett.*, 2003, **44**, 8975–8977.

66 K. Surendra, N. S. Krishnaveni and K. R. Rao, *Synlett*, 2005, **3**, 506–510.

67 K. Samanta and G. Panda, *Org. Biomol. Chem.*, 2011, **9**, 7365.

68 S. Uesugi, T. Watanabe, T. Imaizumi, M. Shibuya, N. Kanoh and Y. Iwabuchi, *Org. Lett.*, 2014, **16**, 4408–4411.

69 D. Li, J. Wang, S. Yu, S. Ye, W. Zou, H. Zhang and J. Chen, *Chem. Commun.*, 2020, **56**, 2256–2259.

70 C. Wang and H. Yamamoto, *J. Am. Chem. Soc.*, 2014, **136**, 6888–6891.

71 A. Kumar and G. Panda, *Tetrahedron Lett.*, 2021, **70**, 153013.

72 C. Wang and H. Yamamoto, *Angew. Chem.*, 2014, **126**, 14140–14143.

73 L. Luo and H. Yamamoto, *Org. Biomol. Chem.*, 2015, **13**, 10466–10470.

74 B. Weber, *Synthesis*, 1999, 1593–1606.

75 H. Li, A. He, J. R. Falck and L. S. Liebeskind, *Org. Lett.*, 2011, **13**, 3682–3685.

76 B. F. Bonini, M. Comes-Franchini, M. Fochi, L. Lunazzi, A. Mazzanti, A. Ricci and G. Varchi, *Synlett*, 2001, **2001**, 995–998.



77 F. Benedetti, F. Berti, S. Budal, P. Campaner, F. Dinon, A. Tossi, R. Argirova, P. Genova, V. Atanassov and A. Hinkov, *J. Med. Chem.*, 2012, **55**, 3900–3910.

78 Z. Liu, H.-S. Byun and R. Bittman, *J. Org. Chem.*, 2011, **76**, 8588–8598.

79 K. S. Olivier and M. S. Van Nieuwenhze, *Org. Lett.*, 2010, **12**, 1680–1683.

80 E. N. Jacobsen, *Acc. Chem. Res.*, 2000, **33**, 421–431.

81 G. Sabitha, R. S. Babu, M. Rajkumar and J. S. Yadav, *Org. Lett.*, 2002, **4**, 343–345.

82 X. E. Hu, *Tetrahedron*, 2004, **60**, 2701–2743.

83 S. Dinda, S. Das and G. Panda, *Synthesis*, 2009, **2009**, 1886–1896.

84 S. K. Das and G. Panda, *Tetrahedron*, 2008, **64**, 4162–4173.

85 P. M. Manoury, J. L. Binet, J. Rousseau, F. M. Lefevre-Borg and I. G. Cavero, *J. Med. Chem.*, 1987, **30**, 1003–1011.

86 C.-L. J. Wang, W. A. Gregory and M. A. Wuonola, *Tetrahedron*, 1989, **45**, 1323–1326.

87 W. A. Gregory, D. R. Brittelli, C. L. J. Wang, M. A. Wuonola, R. J. McRipley, D. C. Eustice, V. S. Eberly, A. M. Slee, M. Forbes and P. T. Bartholomew, *J. Med. Chem.*, 1989, **32**, 1673–1681.

88 R. Giani, E. Marinone, G. Melillo, M. Borsa and G. C. Tonon, *Arzneimittelforschung*, 1988, **38**, 1139–1141.

89 T. Minh Le and Z. Szakonyi, *Chem. Rec.*, 2022, **22**, e202100194.

90 N. Azizi, B. Mirmashhori and M. R. Saidi, *Catal. Commun.*, 2007, **8**, 2198–2203.

91 S. Wang, Z. Xie, M. Li and C. Wang, *ChemistrySelect*, 2020, **5**, 6011–6015.

92 T. M. Le, T. Huynh, G. Endre, A. Szekeres, F. Fülöp and Z. Szakonyi, *RSC Adv.*, 2020, **10**, 38468–38477.

93 L. Ciccone, G. Petrarolo, F. Barsuglia, C. Fruchart-Gaillard, E. Cassar Lajeunesse, A. T. Adewumi, M. E. S. Soliman, C. La Motta, E. Orlandini and S. Nencetti, *Biomolecules*, 2022, **12**, 448.

94 T. M. Le, T. Huynh, F. Z. Bamou, A. Szekeres, F. Fülöp and Z. Szakonyi, *Int. J. Mol. Sci.*, 2021, **22**, 5626.

95 D. Friedrich and F. Bohlmann, *Tetrahedron*, 1988, **44**, 1369–1392.

96 D. Bai, Z. Schelz, D. Erdős, A. K. Kis, V. Nagy, I. Zupkó, G. T. Balogh and Z. Szakonyi, *Int. J. Mol. Sci.*, 2023, **24**, 1121.

97 D. A. DeGoey, H.-J. Chen, P. B. Cox and M. D. Wendt, *J. Med. Chem.*, 2018, **61**, 2636–2651.

98 B. C. Doak, B. Over, F. Giordanetto and J. Kihlberg, *Chem. Biol.*, 2014, **21**, 1115–1142.

99 C. A. Lipinski, F. Lombardo, B. W. Dominy and P. J. Feeney, *Adv. Drug Delivery Rev.*, 1997, **23**, 3–25.

100 D. F. Veber, S. R. Johnson, H.-Y. Cheng, B. R. Smith, K. W. Ward and K. D. Kopple, *J. Med. Chem.*, 2002, **45**, 2615–2623.

101 T. W. Johnson, R. A. Gallego and M. P. Edwards, *J. Med. Chem.*, 2018, **61**, 6401–6420.

102 B. R. Travis, R. S. Narayan and B. Borhan, *J. Am. Chem. Soc.*, 2002, **124**, 3824–3825.

103 F. Wohnsland and B. Faller, *J. Med. Chem.*, 2001, **44**, 923–930.

104 T. Mosmann, *J. Immunol. Methods*, 1983, **65**, 55–63.

